

**Dixenite, $\text{Cu}^{1+}\text{Mn}_{14}^{2+}\text{Fe}^{3+}(\text{OH})_6(\text{As}^{3+}\text{O}_3)_5(\text{Si}^{4+}\text{O}_4)_2(\text{As}^{5+}\text{O}_4)$:
metallic $[\text{As}_4^{3+}\text{Cu}^{1+}]$ clusters in an oxide matrix**

TAKAHARU ARAKI AND PAUL B. MOORE

*Department of the Geophysical Sciences
The University of Chicago, Chicago, Illinois 60637*

Abstract

The crystal structure of dixenite was analyzed using a crystal from the type and sole locality at Långban, Sweden. The end-member formula $\text{Cu}^{1+}\text{Mn}_{14}^{2+}\text{Fe}^{3+}(\text{OH})_6(\text{As}^{3+}\text{O}_3)_5(\text{Si}^{4+}\text{O}_4)_2(\text{As}^{5+}\text{O}_4)$ is proposed. Dixenite is rhombohedral, $a = 8.233(4)$, $c = 37.499(1)\text{\AA}$, space group $R\bar{3}$, $Z = 3$. Twenty eight atoms occur in the asymmetric unit including two disordered Cu^{1+} cations. $R = 0.064$ for 2507 independent reflections.

The structure is related to but distinct from that of hematolite, $(\text{Mn}^{2+}, \text{Mg}, \text{Al})_{15}(\text{OH})_{23}(\text{AsO}_3)(\text{AsO}_4)_2$. Three kinds of anionic radicals occur: $(\text{As}^{3+}\text{O}_3)$ trigonal pyramids; and $(\text{Si}^{4+}\text{O}_4)$ and $(\text{As}^{5+}\text{O}_4)$ tetrahedra. Three of the five nonequivalent layers along [001] are similar in hematolite and dixenite. One layer in dixenite, however, contains a disordered cluster, idealized as $(\text{Cu}^{1+}\text{As}_4^{3+})$ where a tetrahedron of As^{3+} ions surrounds a Cu^{1+} ion. All lone pair electrons from As^{3+} point into the central cavity which houses $\text{Cu}^{1+}(d^{10})$ and this cluster is believed to be stabilized by the 18-electron rule where $\text{Cu}^{1+}\text{As}_4^{3+}$ forms a closed argon core.

Introduction

Dixenite is a rare mineral, originally described by Flink (1920) from the mineralogically complex Fe–Mn oxide ore deposit in Långban, Sweden. The mineral was long problematical: Wickman (1951) proposed the formula $(\text{Mn}, \text{Fe}, \text{Cu}, \text{As}^{3+})_{20}(\text{Si}, \text{As}^{5+})_3(\text{O}, \text{OH})_{32}$, Wuensch (1960) presented a relationship to the complex arsenosilicate mcgovernite, and Moore and Araki (1978) proposed $\text{Mn}_{11}^{2+}\text{Mn}_4^{3+}(\text{OH})_8(\text{AsO}_3)_6(\text{SiO}_4)_2$ and a model for the structure derived from hematolite, $(\text{Mn}^{2+}, \text{Mg}, \text{Al})_{15}(\text{OH})_{23}(\text{AsO}_3)(\text{AsO}_4)_2$ to which it shares similarities in cell parameters and space group.

We studied dixenite's structure in hopes of gathering more clues about the structure of mcgovernite, and discovered several unusual features, including incorrectness of the proposed structure of Moore and Araki (1978), the presence of $[\text{As}_4^{3+}\text{Cu}^{1+}]$ metal clusters, the occurrence of As^{3+}O_3 trigonal pyramids, and solid solution between As^{4+} and Si^{4+} in tetrahedral oxygen coordination.

Experimental details

On the basis of a relationship to hematolite, kraisslite and mcgovernite (Moore and Ito, 1978) we

suspected that platy deep red-brown crystals of dixenite from the only recorded locality at Långban, Sweden may in fact consist of more than one structure or polytype. Our dixenite sample selected for this structure study was NMNH No. C-6440. We also examined Nos. B-20579, 94920, 94935 and R-5755 (all in the U.S. National Museum of Natural History) by X-ray study and found all of them to be identical. We thank Mr. John S. White, Jr. for permission to select fragments of these specimens. The crystal selected was a deep red plate measuring $0.18\text{ mm} \parallel a_1 \times 0.25\text{ mm} \parallel a_2 \times 0.06\text{ mm} \parallel c$. With $\mu = 132.1\text{ cm}^{-1}$ ($\text{MoK}\alpha$), seven divisions by the Gaussian integral method (Burnham, 1966) led to significant absorption corrections, ranging from 0.148 for low angle (00l) reflections to 0.458.

Cell data were obtained from calibrated precession photographs ($\text{MoK}\alpha$ radiation) and yielded $a = 8.233(4)$, $c = 37.499(1)\text{\AA}$, Laue symmetry 3. Intensities were collected on a PAILRED semi-automated diffractometer with the a_2 -axis \parallel rotation and with graphite monochromatized $\text{MoK}\alpha$ radiation. Background counting time on each side of the peak was 20 sec, scan speed 1° min^{-1} , scan width 4.0° to 4.8° . Angular coverage maximum was $\sin\theta/\lambda = 0.80$, the

Table 1. Dixenite: atomic coordinate parameters[†]

Atom	Population	x	y	z
M(1)	1.0Mn ²⁺	0	0	0
M(2)	0.90(2)Mn ²⁺ + 0.10(2)Mg ²⁺	1/3	2/3	0.0622(9)
M(3)	1.0Fe ³⁺	0	0	0.25749(7)
M(4)	1.0Mn ²⁺	0.0408(1)	0.2617(1)	0.06782(6)
M(5)	1.0Mn ²⁺	0.4158(2)	0.3359(2)	0.12987(6)
M(6)	1.0Mn ²⁺	0.1089(1)	0.3976(1)	0.19230(6)
M(7)	1.0Mn ²⁺	0.4226(1)	0.3154(1)	0.26133(6)
Cu(1)	0.651(9)Cu ¹⁺ + 0.349□	1/3	2/3	0.31292(9)
Cu(2)	0.192(9)Cu ¹⁺ + 0.808□	2/3	1/3	0.0050(3)
T(1)	0.86(1)Si ⁴⁺ + 0.14As ⁵⁺	2/3	1/3	0.18792(9)
T(2)	0.60(1)Si ⁴⁺ + 0.40As ⁵⁺	0	0	0.14620(7)
T(3)	0.24(1)Si ⁴⁺ + 0.76As ⁵⁺	1/3	2/3	0.11357(6)
As(1)	1.0As ³⁺	2/3	1/3	0.06992(6)
As(2)	1.0As ³⁺	1/3	2/3	0.25062(6)
As(3)	1.0As ³⁺	0.08854(9)	0.37369(9)	0.31589(6)
O(1)		0	0	0.1019(2)
O(2)		1/3	2/3	0.1584(3)
O(3)		2/3	1/3	0.2311(2)
O(4)		0.0899(7)	0.4444(7)	0.0212(2)
O(5)		0.4698(7)	0.1659(7)	0.0949(1)
O(6)		0.2837(7)	0.4545(7)	0.0988(2)
O(7)		0.1655(7)	0.2081(6)	0.1617(1)
O(8)		0.5194(7)	0.1277(7)	0.1707(1)
O(9)		0.3690(7)	0.5010(7)	0.2277(1)
O(10)		0.1468(7)	0.2272(7)	0.2905(1)
O(11)		0.4608(6)	0.1185(7)	0.2956(1)
OH(1)		0.2140(7)	0.1791(7)	0.0375(2)
OH(2)		0.2352(7)	0.0814(7)	0.2271(1)

[†]Estimated standard errors refer to the last digit.

highest level $k = 11$. A total of 4989 reflections was covered including (hkl) , $(h\bar{k}l)$, $(h+l, h, l)$ and $(h+k, h, \bar{l})$. Unobserved reflections with $I_0 < 2\sigma(I)$ accounted for 397 (8%) of the total reflections.

Equivalent reflection pairs, such as (hkl) and $(h+k, h, l)$ were found to have equivalent intensities within error of observation after absorption correction and were therefore averaged. The Bijvoet pairs were preserved in the data set owing to pronounced acentricity, as determined with an $N(z)$ test on general reflections (Howells *et al.*, 1950). The space group is therefore $R3$. A total of 2507 independent reflections were used in the ensuing study.

Solution and refinement of the structure

The dixenite model proposed by Moore and Araki (1978) and derived from the structure of hematolite, a basic manganese arsenite-arsenate which has similar cell parameters, was first tested and found to be incorrect. The structure was solved piecemeal, with stepwise approach by Fourier methods starting with atomic positions which satisfied the most prominent vectors of a Patterson synthesis. The problem of structure analysis proved to be exceedingly complicated, the results of which require an extensive revision of dixenite's proposed formula. Much like magnussonite (Moore and Araki, 1979a), a cluster of As^{3+} cations appeared, the core of which afforded two electron density maxima. Like magnussonite, the distances between

As^{3+} and these maxima were short ($< 2.7\text{\AA}$) and we anticipated "metal-metal" bonding. Unlike magnussonite, the As^{3+} defined a tetrahedral array, *not* an octahedral array. We assumed a similar mechanism operated in dixenite, *i.e.*, the 18-electron rule and observed that sufficient Cu^{1+} was present to account for this residual density. Counting valence electrons there exist $2 \times 4(As^{3+}) + 10(d^{10}$ in $Cu^{1+})$ binding the cluster, defining a closed argon core. At this stage, we suspected that Cu^{1+} reported in some magnussonite analyses may in fact occur in the center of the As_6^{3+} octahedron in that structure but no sensible electron "rule" could be extracted from this model. Solid solutions and partly occupied sites required application of mixed scattering curves [$xSi^{4+} + (1-x)As^{5+}$] and ordered vacancies [$yCu^{1+} + (1-y)\square$, where \square = vacancy]. Several cycles of atomic coordinate parameter, site population and anisotropic thermal vibration parameter refinement led to $R = 0.064$, and $R_w = 0.065$ for 2507 independent reflections where

$$R = \frac{\sum |F_0| - |F_c|}{\sum |F_0|} \text{ and } R_w = \left[\frac{\sum w(|F_0| - |F_c|)^2}{\sum w|F_0|^2} \right]^{1/2}$$

with $w = \sigma^{-2}$ of F_0 . Refinement minimized $w(F_0 - F_c)^2$. Programs used in this study have been listed

Table 2. Dixenite: anisotropic thermal vibration parameters[†]

Atom	β_{11}	β_{22}	β_{33}	β_{12}	β_{13}	β_{23}
M(1)	46(2)	46	12(1)	23	0	0
M(2)	48(4)	48	41(2)	24	0	0
M(3)	28(2)	28	14(1)	14	0	0
M(4)	41(2)	51(2)	16(1)	24(1)	-0(0)	-2(0)
M(5)	45(2)	61(2)	18(1)	29(1)	-1(0)	-4(0)
M(6)	42(2)	42(2)	18(1)	22(1)	-2(0)	-1(0)
M(7)	35(2)	35(2)	15(1)	19(1)	-1(0)	0(0)
Cu(1)	29(4)	29	19(2)	15	0	0
Cu(2)	38(14)	38	30(7)	19	0	0
T(1)	32(5)	32	9(2)	16	0	0
T(2)	30(3)	30	10(1)	15	0	0
T(3)	29(2)	29	8(1)	15	0	0
As(1)	38(2)	38	9(1)	19	0	0
As(2)	37(2)	37	10(1)	18	0	0
As(3)	35(1)	42(1)	12(1)	23(1)	-0(0)	-0(0)
O(1)	64(14)	64	14(5)	32	0	0
O(2)	60(14)	60	18(6)	30	0	0
O(3)	35(11)	35	10(5)	18	0	0
O(4)	72(9)	55(9)	14(3)	28(7)	-1(1)	1(1)
O(5)	34(7)	32(7)	19(3)	12(6)	-2(1)	-3(1)
O(6)	45(8)	39(7)	23(3)	30(7)	-4(1)	-2(1)
O(7)	40(7)	26(7)	18(3)	17(6)	0(1)	-2(1)
O(8)	37(7)	45(8)	11(3)	11(6)	2(1)	-1(1)
O(9)	50(8)	50(8)	15(3)	34(7)	-2(1)	0(1)
O(10)	49(8)	39(7)	19(3)	25(6)	0(1)	-2(1)
O(11)	27(7)	34(7)	14(3)	1(6)	1(1)	2(1)
OH(1)	44(8)	47(8)	17(3)	19(7)	-2(1)	-2(1)
OH(2)	50(8)	40(7)	14(3)	25(6)	-1(1)	-1(1)

[†]Coefficients in the expression $\exp[-\beta_{11}h^2 + \beta_{22}k^2 + \beta_{33}l^2 + 2\beta_{12}hk + 2\beta_{13}hl + 2\beta_{23}kl]$. Estimated standard errors refer to the last digit. The coefficient β_{33} is $\times 10^3$, the others each $\times 10^4$.

Table 3. Dixenite: parameters for the ellipsoids of vibration[†]

Atom	<i>i</i>	μ_i	θ_{i_a}	θ_{i_b}	θ_{i_c}	Beq(\AA^2)	Atom	<i>i</i>	μ_i	θ_{i_a}	θ_{i_b}	θ_{i_c}	Beq(\AA^2)
M(1)	1	0.093(4)	90	90	0	0.85(3)	As(3)	1	0.089(1)	10(90)	126(70)	82(33)	0.72(1)
	2	0.109(4)	***** not determined	*****	*****			2	0.092(1)	84(20)	105(14)	165(8)	
	3	0.109(4)	***** not determined	*****	*****			3	0.105(1)	98(4)	140(8)	77(4)	
M(2)	1	0.112(6)	***** not determined	*****	*****	1.43(7)	O(1)	1	0.101(19)	90	90	0	1.13(18)
	2	0.112(6)	***** not determined	*****	*****			2	0.128(19)	***** not determined	*****	*****	
	3	0.171(4)	90	90	0			3	0.128(19)	***** not determined	*****	*****	
M(3)	1	0.086(5)	***** not determined	*****	*****	0.66(3)	O(2)	1	0.114(19)	90	90	0	1.15(17)
	2	0.086(5)	***** not determined	*****	*****			2	0.124(19)	***** not determined	*****	*****	
	3	0.101(4)	90	90	0			3	0.124(19)	***** not determined	*****	*****	
M(4)	1	0.092(2)	120(12)	52(8)	41(11)	0.91(1)	O(3)	1	0.085(20)	90	90	0	0.67(14)
	2	0.102(2)	146(14)	90(7)	106(7)			2	0.095(20)	***** not determined	*****	*****	
	3	0.125(2)	76(4)	142(5)	54(4)			3	0.095(20)	***** not determined	*****	*****	
M(5)	1	0.097(2)	103(14)	53(10)	38(8)	1.04(2)	O(4)	1	0.097(11)	81(10)	104(19)	14(14)	1.16(7)
	2	0.104(2)	166(90)	72(5)	97(14)			2	0.120(9)	93(17)	146(35)	100(19)	
	3	0.139(2)	85(3)	137(5)	53(2)			3	0.143(8)	170(90)	59(40)	80(18)	
M(6)	1	0.097(2)	55(30)	77(24)	56(7)	0.89(2)	O(5)	1	0.077(12)	71(17)	55(19)	64(10)	0.84(7)
	2	0.100(2)	41(90)	160(90)	96(29)			2	0.105(9)	19(90)	136(90)	99(42)	
	3	0.120(2)	108(4)	106(5)	35(5)			3	0.123(9)	89(23)	114(22)	28(12)	
M(7)	1	0.087(2)	33(31)	128(21)	60(14)	0.74(1)	O(6)	1	0.076(12)	31(90)	144(78)	75(26)	0.93(7)
	2	0.095(2)	102(10)	138(27)	97(7)			2	0.099(10)	107(18)	125(27)	119(10)	
	3	0.107(2)	121(6)	75(8)	31(9)			3	0.141(9)	115(7)	95(8)	33(11)	
Cu(1)	1	0.087(8)	***** not determined	*****	*****	0.76(7)	O(7)	1	0.073(12)	108(22)	22(63)	71(17)	0.78(6)
	2	0.087(8)	***** not determined	*****	*****			2	0.101(9)	26(44)	97(20)	101(27)	
	3	0.117(6)	90	90	0			3	0.118(9)	73(26)	111(13)	23(22)	
Cu(2)	1	0.101(24)	***** not determined	*****	*****	1.10(24)	O(8)	1	0.074(13)	123(11)	81(14)	35(23)	0.86(7)
	2	0.101(24)	***** not determined	*****	*****			2	0.097(10)	112(19)	122(15)	113(17)	
	3	0.146(18)	90	90	0			3	0.133(9)	42(36)	146(45)	66(20)	
T(1)	1	0.081(7)	90	90	0	0.61(7)	O(9)	1	0.077(12)	41(33)	132(28)	56(27)	0.88(7)
	2	0.091(9)	***** not determined	*****	*****			2	0.111(10)	75(28)	133(22)	137(35)	
	3	0.091(9)	***** not determined	*****	*****			3	0.122(9)	127(21)	107(28)	67(26)	
T(2)	1	0.083(5)	90	90	0	0.58(5)	O(10)	1	0.083(11)	115(21)	30(40)	60(20)	0.93(7)
	2	0.087(6)	***** not determined	*****	*****			2	0.112(9)	30(48)	90(21)	91(29)	
	3	0.087(6)	***** not determined	*****	*****			3	0.125(9)	75(32)	120(15)	30(28)	
T(3)	1	0.077(4)	90	90	0	0.55(4)	O(11)	1	0.068(13)	122(17)	115(11)	72(11)	0.82(6)
	2	0.086(5)	***** not determined	*****	*****			2	0.102(10)	113(19)	83(18)	156(15)	
	3	0.086(5)	***** not determined	*****	*****			3	0.127(9)	139(69)	26(90)	75(34)	
As(1)	1	0.079(3)	90	90	0	0.68(2)	OH(1)	1	0.091(11)	73(19)	62(18)	49(17)	0.97(7)
	2	0.098(3)	***** not determined	*****	*****			2	0.114(9)	20(90)	122(42)	110(47)	
	3	0.098(3)	***** not determined	*****	*****			3	0.125(9)	79(41)	135(49)	47(22)	
As(2)	1	0.083(3)	90	90	0	0.67(2)	OH(2)	1	0.090(11)	107(30)	41(52)	50(45)	0.84(7)
	2	0.097(3)	***** not determined	*****	*****			2	0.103(10)	121(45)	49(47)	137(49)	
	3	0.097(3)	***** not determined	*****	*****			3	0.114(9)	143(60)	95(24)	77(26)	

[†] *i* = *i*th principal axis, μ_i = rms amplitude, θ_{i_a} , θ_{i_b} , θ_{i_c} = angles (deg.) between the *i*th principal axis and the cell axes *a*₁, *a*₂, and *a*₃. The equivalent isotropic thermal vibration parameter, Beq, is also listed. Estimated standard errors in parentheses refer to the last digit.

earlier (Moore and Araki, 1976). Scattering curves for Mn²⁺, Cu²⁺, Mg²⁺, As⁰⁺, Si⁴⁺ and O¹⁻ were obtained from Cromer and Mann (1968) and anomalous dispersion corrections, *f''*, for all metals from Cromer and Liberman (1970).

Reasonable errors in bond distances ($\pm 0.005\text{\AA}$ for metal-oxygen distances), sensible equivalent isotropic thermal parameters ($< 1.4\text{\AA}^2$), good agreement with observed specific gravity and chemical plausibility support our findings on this unusual structure and demonstrate yet again that crystal structure analysis may be required to establish a meaningful chemical formula.

Atomic coordinate parameters are given in Table 1, anisotropic thermal vibration parameters in Table 2, thermal vibration ellipsoids and equivalent iso-

tropic thermal parameters in Table 3, structure factor tables in Table 4,¹ bond distances and angles in Table 5, select chemical analyses in Table 6 and bond length-bond strength relations in Table 7.

Discussion of the structure

Table 6 presents cell contents based on the structure analysis and on the Johansson analysis in Wickman (1951). The agreement is excellent and demonstrates the importance of structure study in ascribing formal charges. From the structure study,

¹ To obtain a copy of Table 4, order Document AM-81-181 from the Business Office, Mineralogical Society of America, 2000 Florida Avenue, N.W., Washington, D.C. 20009. Please remit \$1.00 in advance for the microfiche.

Table 5. Dixenite: bond distances and angles[†]

Cu(1)			As(1)		
3 Cu(1) ⁽³⁾ -As(3) ⁽³⁾	2.240(1) Å		3 As(1)-O(5)	1.779(5)	
1 Cu(1) ⁽³⁾ -As(2) ⁽³⁾	2.336(3)		3 O(5)-O(5) ⁽¹⁾	2.619(8)**	94.8(2)
average	2.264				
		Angle (°)			
3 As(2) ⁽³⁾ -As(3) ⁽³⁾	3.316(1)	92.85(7)	As(2)		
3 As(3) ⁽³⁾ -As(3) ⁽⁴⁾	3.875(1)	119.75(1)	3 As(2)-O(9)	1.755(5)	
average	3.595	106.3	3 O(9)-O(9) ⁽¹⁾	2.650(8)**	98.0(2)
Cu(2)			As(3)		
3 Cu(2)-As(3) ⁽³⁾	2.365(4)		As(3)-O(4) ⁽⁸⁾	1.721(5)	
1 Cu(2)-As(1)	2.510(10)		-O(11) ⁽¹⁾	1.762(5)	
average	2.401		-O(10)	1.779(5)	
3 As(3) ⁽³⁾ -As(3) ⁽⁴⁾	3.875(1)	110.0(2)	average	1.754	
3 As(1)-As(3) ⁽³⁾	3.967	108.9(3)	0(4) ⁽⁸⁾ -O(10)	2.643(7)**	98.1(3)
average	3.921	109.5	0(10)-O(11) ⁽¹⁾	2.785(7)	103.8(2)
			0(4) ⁽⁸⁾ -O(11) ⁽¹⁾	2.792(7)	106.6(3)
			average	2.740	102.8
M(1)					
3 M(1)-OH(1)	2.157(5) Å		T(1)		
3 M(1)-O(11) ⁽³⁾	2.235(5)		1 T(1)-O(3)	1.620(9)	
average	2.196		3 T(1)-O(8)	1.641(5)	
3 OH(1)-OH(1) ⁽¹⁾	2.832(8)*	82.0(2)	average	1.636	
3 O(11) ⁽³⁾ -O(11) ⁽⁴⁾	2.998(8)*	84.2(2)	3 O(8)-O(8) ⁽¹⁾	2.614(9)	105.5(2)
3 OH(1)-O(11) ⁽⁴⁾	3.151(7)	91.7(2)	3 O(3)-O(8)	2.722(9)	113.2(2)
3 OH(1)-O(11) ⁽⁵⁾	3.432(7)	102.7(2)	average	2.668	109.4
average	3.103	90.1			
M(2)					
3 M(2)-O(4)	2.001(5)		T(2)		
3 M(2)-O(10) ⁽³⁾	2.464(6)		1 T(2)-O(1)	1.662(9)	
average	2.232		3 T(2)-O(7)	1.669(5)	
3 O(4)-O(10) ⁽⁴⁾	2.643(7)**	71.7(2)	average	1.667	
3 O(10) ⁽³⁾ -O(10) ⁽⁴⁾	2.842(9)*	70.4(2)	3 O(7)-O(7) ⁽¹⁾	2.712(8)	108.6(2)
3 O(4)-O(4) ⁽¹⁾	3.327(9)	112.4(2)	3 O(1)-O(7)	2.734(9)	110.3(2)
3 O(4)-O(10) ⁽⁵⁾	3.403(8)	98.8(2)	average	2.723	109.4
average	3.054	88.3			
M(3)					
3 M(3)-OH(2)	2.048(5)		T(3)		
3 M(3)-O(10)	2.056(5)		3 T(3)-O(6)	1.675(5)	
average	2.052		1 T(3)-O(2)	1.681(10)	
3 O(10)-O(10) ⁽¹⁾	2.842(9)*	87.4(2)	average	1.676	
3 O(10)-OH(2) ⁽²⁾	2.901(7)	90.0(2)	3 O(2)-O(6)	2.738(9)	109.3(2)
3 OH(2)-O(10)	2.915(7)*	90.5(2)	3 O(6)-O(6) ⁽¹⁾	2.738(8)	109.6(2)
3 OH(2)-OH(2) ⁽¹⁾	2.946(9)	92.0(2)	average	2.738	109.4
average	2.901	90.0			

[†]Estimated standard errors in parentheses refer to the last digit. The equivalent positions (referred to Table 1) are designated as superscripts and are (1) = -y, x-y, z; (2) = y-x, -x, z; (3) = (1/3 2/3 2/3) + (x, y, z); (4) = (1/3 2/3 2/3) + (-y, x-y, z); (5) = (1/3 2/3 2/3) + (y-x, -x, z).

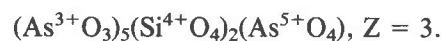
*0-0° shared edges between octahedra. **0-0° shared edges between octahedron and trigonal pyramid.

Table 5 (continued)

M(4)			M(6)		
M(4)-O(5) ⁽¹⁾	2.152(5)		M(6)-O(8) ⁽¹⁾	2.086(5)	
-OH(1) ⁽¹⁾	2.160(5)		-O(7)	2.166(5)	
-O(6)	2.165(5)		-OH(2) ⁽¹⁾	2.244(5)	
-OH(1)	2.178(5)		-O(9) ⁽²⁾	2.262(5)	
-O(4)	2.207(5)		-O(9)	2.289(5)	
-O(1)	2.377(5)		-O(2)	2.415(5)	
average	2.206		average	2.244	
OH(1)-OH(1) ⁽¹⁾	2.832(8)*	81.5(3)	O(9)-O(9) ⁽²⁾	2.650(8)**	71.2(3)
O(4)-OH(1)	2.898(7)	82.7(2)	O(8) ⁽¹⁾ -O(9) ⁽²⁾	2.967(7)	86.0(2)
O(1)-OH(1) ⁽¹⁾	2.915(9)*	79.8(2)	O(2)-O(9)	3.015(9)*	79.7(2)
O(1)-OH(1)	2.915(9)*	79.4(2)	O(2)-O(9) ⁽²⁾	3.015(9)*	80.2(2)
O(4)-OH(1) ⁽¹⁾	3.026(8)	87.7(2)	O(8) ⁽¹⁾ -OH(2) ⁽¹⁾	3.031(7)	88.8(2)
O(5) ⁽¹⁾ -OH(1) ⁽¹⁾	3.048(7)	90.0(2)	O(7)-OH(2) ⁽¹⁾	3.071(7)	88.3(2)
O(6)-OH(1)	3.072(7)	90.0(2)	O(7)-O(9)	3.272(7)	94.5(2)
O(5) ⁽¹⁾ -O(6)	3.130(7)	98.2(2)	O(2)-O(7)	3.307(5)	92.3(2)
O(1)-O(6)	3.272(5)	92.0(2)	O(2)-O(8) ⁽¹⁾	3.336(5)	95.4(2)
O(4)-O(6)	3.298(7)	98.0(2)	O(9)-OH(2) ⁽¹⁾	3.361(7)	95.7(2)
O(4)-O(5) ⁽¹⁾	3.311(7)	98.9(2)	O(9) ⁽²⁾ -OH(2) ⁽¹⁾	3.405(7)	98.2(2)
O(1)-O(5) ⁽¹⁾	3.404(5)	97.3(2)	O(7)-O(8) ⁽¹⁾	3.442(7)	108.1(2)
average	3.093	89.6	average	3.156	89.9
M(5)			M(7)		
M(5)-O(8) ⁽²⁾	2.093(5)		M(7)-OH(2)	2.182(5)	
-O(5)	2.120(5)		-O(9)	2.188(5)	
-O(6)	2.133(5)		-O(11)	2.210(5)	
-O(7)	2.145(5)		-O(3)	2.245(5)	
			-O(11) ⁽²⁾	2.284(5)	
-O(5) ⁽²⁾	2.429(5)		-O(10)	2.285(5)	
			average	2.232	
-O(8)	2.730(5)				
average (inner four)	2.123		O(10)-OH(2)	2.915(7)*	81.4(2)
average (inner five)	2.184		O(3)-O(11)	2.974(8)*	83.8(2)
average (six)	2.275		O(3)-O(11) ⁽²⁾	2.974(8)*	82.1(2)
			O(11)-O(11) ⁽²⁾	2.998(8)*	83.7(3)
Inner four anions			O(9)-OH(2)	3.053(7)	88.6(2)
O(6)-O(7)	2.939(7)	86.8(2)	O(3)-OH(2)	3.091(5)	88.6(2)
O(7)-O(8) ⁽²⁾	3.120(7)	98.1(2)	O(11)-OH(2)	3.094(7)	89.6(2)
O(5)-O(6)	3.410(7)	106.6(2)	O(10)-O(11)	3.132(7)	88.3(2)
O(5)-O(8) ⁽²⁾	3.623(7)	118.6(2)	O(9)-O(10)	3.138(7)	89.1(2)
O(5)-O(7)	3.677(7)	119.2(2)	O(3)-O(9)	3.359(5)	98.5(2)
O(6)-O(8) ⁽²⁾	3.724(7)	123.6(2)	O(9)-O(11) ⁽²⁾	3.388(7)	98.5(2)
average	3.416	108.8	O(10)-O(11) ⁽²⁾	3.673(7)	107.0(2)
			average	3.149	89.9

we accepted Cu^{1+} , Mn^{2+} , As^{3+} and As^{5+} as formal charges, then recalculated Johansson's analysis to accommodate these differences which resulted in a negligible amount of Mn^{3+} . From the structure study, we obtain $\text{Mn}_{42.13}^{2+}\text{Mg}_{0.30}^{2+}\text{Fe}_{2.57}^{3+}\text{As}_{15.00}^{3+}\text{Cu}_{2.53}^{1+}\text{Si}_{5.10}^{4+}\text{As}_{3.90}^{5+}(\text{OH})_{18}\text{O}_{81}$ in the cell. This gives $\rho(\text{calc}) = 4.375 \text{ g cm}^{-3}$ in excellent agreement with the specific gravity of 4.36 reported in Wickman (1951). From this exceedingly complex formula a

unit formula is proposed for an ideal "end-member" composition (*vide supra*):



This formula disguises the peculiar aspects of dixenite's crystal chemistry: first Si^{4+} and As^{5+} mix over their sites, and second the Johansson analysis

Table 6. Dixenite: chemical analysis and its interpretation

	1	2	3		4	5
P ₂ O ₅	0.02	-	-	P ⁵⁺	-	-
As ₂ O ₅	-	7.74	5.96	As ⁵⁺	3.90	3.90
SiO ₂	5.31	5.30	6.23	Si ⁴⁺	5.10	5.13
As ₂ O ₃	32.16	25.64	25.65	As ³⁺	15.00	14.97
Mn ₂ O ₃	8.05	-	-	Mn ³⁺	-	0.66
Fe ₂ O ₃	3.75	3.55	4.14	Fe ³⁺	2.57	2.73
MgO	0.32	0.21	-	Mg ²⁺	0.30	0.46
MnO	43.35	51.63	51.51	Mn ²⁺	42.13	40.73
CaO	0.39	-	-	Ca ²⁺	-	0.41
CuO	3.49	-	-	Cu ²⁺	-	-
Cu ₂ O	-	3.13	3.71	Cu ¹⁺	2.53	2.55
Na ₂ O	0.13	-	-			
K ₂ O	0.14	-	-			
H ₂ O	2.80	2.80	2.80			
Total	99.91	100.00	72.00	Σ Atoms	71.53	71.54
			180.00	Σ Charge	180.00	180.85
Specific gravity	4.36					
Density (g cm ⁻³)		4.375				

¹Johansson analysis in Wickman (1951).

²Calculated weight percent from structure study and from column 4.

³For proposed end-member composition Cu¹⁺Mn²⁺Fe³⁺(AsO₃)₅(SiO₄)₂(AsO₄)(OH)₆.

⁴Cell contents of cations computed from structure analysis. Total Fe³⁺ was computed to exactly balance anion charge = 180 electrons.

⁵Cell contents of cations computed from Johansson analysis and converting Cu²⁺ + Cu¹⁺:As³⁺ + As⁵⁺; As³⁺ + As⁵⁺:Mn³⁺ + Mn²⁺ in that order, the Cu¹⁺ and As⁵⁺ totals dictated from the structure study.

suggests a slight deficit of cations which in Table 6 appears to result from less As⁵⁺ and more Si⁴⁺ and somewhat less Cu¹⁺ in his analysis. However, the table demonstrates very good agreement with the "end-member" formula.

The most interesting feature of the structure is a metallic cluster, ideally [As₄³⁺Cu¹⁺] where the Cu¹⁺ is coordinated by four As³⁺ at the vertices of a distorted tetrahedron, the lone-pair electrons pointing into the central Cu¹⁺ cation. This feature was a surprise in the structure study but it is interesting to note that minerals coexisting with dixenite include native lead, Pb⁰; α-domeykite, α-Cu₃As and magnussonite, Mn₉²⁺Cl[As₆³⁺Mn¹⁺O₁₈]. Magnussonite's structure (Moore and Araki, 1979a) evidently consists of a metallic cluster [As₆³⁺Mn¹⁺] where the 18-electron rule is also satisfied but the distribution of As³⁺ about Mn¹⁺ defines a distorted octahedron. However, in the more recent study on the related arsenite armangite (Moore and Araki, 1979b) we found a similar distribution of As₆³⁺ but no central metal, thus creating concern over the magnussonite study. However, the excellent convergence of the dixenite refinement, the role of Cu¹⁺ and the appearance of a tetrahedral metallic cluster strongly implies that these "bits of metal" in an oxide matrix are real and that dixenite and coexisting magnussonite are two examples in natural systems which represent a transition between the ionic oxides and the sulfides, sulfosalts and alloy-like phases which

contain strong metallic bonds. The end-member formula emphasizes that Cu¹⁺, and to a lesser extent Fe³⁺, are essential to the structure.

Dixenite is thus, like its relative mcgovernite, a basic arsenite-silicate-arsenate. Its name derived from the occurrence of two strangers—arsenite and silicate radicals—as originally proposed by Flink (1920). But it might better have been called "trixenite" owing to the presence of *three* radicals!

Although the structure cells of dixenite and hematolite are very similar, their contents and layer arrangements are quite different. Moore and Araki (1978) showed that hematolite is based on closest packing of oxygens and presented the five non-equivalent layers as Figures 2a-e and that the stacking sequence is · hhhch · . Using the same layer notation in the Figure 1a-e series in this paper it is seen that the *m*=0 layer in dixenite is quite unlike any layer in hematolite and includes the disordered [As₄³⁺Cu¹⁺] clusters. Even the layer itself is not close-packed as shown by the non-parallel orientation of the M(1) and M(2) octahedra. The *m*=1 layer is the same type as *m*=2 in hematolite. The dixenite *m*=2 layer has no correspondence with hematolite, consisting of T(2) and T(3) tetrahedra and very distorted M(5) polyhedra. The dixenite *m*=3 layer is similar to the *m*=1 layer in hematolite but with T(1)O₄ tetrahedra in place of hematolite's As³⁺O₃ trigonal pyramids. The dixenite *m*=4 layer is similar to hematolite's *m*=1 layer but with As³⁺O₃ trigonal pyramids instead of (AsO₄) tetrahedra. This layer is interesting in that it is the same type of octahedral layer as found in Figure 1a (Horiuchi *et al.*, 1979) while the *m*=3 layer is the same type as their Figure 1b as found in 2Mg₂SiO₄ · 3Mg(OH)₂. Welinite, Mn⁴⁺Mn₃²⁺SiO₇, the simplest of these structures, has an octahedral sheet like the *m*=4 layer in dixenite. What is interesting about this layer is the occurrence of small octahedrally coordinated cations on the special 3-fold axial position: in welinite it is populated by Mn⁴⁺, in hematolite by mixed Al³⁺ and Fe³⁺, in dixenite principally by Fe³⁺(M(3)). For this reason, Fe³⁺ (or possibly Al³⁺) appears to be an important component in the structure.

Bond distances and their deviations

Table 5 lists individual bond distances and angles for the individual coordination polyhedra in dixenite's structure. The individual distances were arranged according to increasing values and shared polyhedral edges are starred. These shared edge

Table 7. Dixenite: electrostatic valence balance of cations and anions[†]

Bond Strength	Coordinating Cations													Δp_0
	M(1)	M(2)	M(3)	M(4)	M(5)	M(6)	M(7)	T(1)	T(2)	T(3)	As(1)	As(2)	As(3)	
	2/6	2/6	3/6	2/6	2/4	2/6	2/6	4.25/4	4.5/4	4.75/4	3/3	3/3	3/3	
Anions														
O(1)	----	----	----	3 <u>+0.17</u> (x3)	----	----	----	----	1 -0.01	----	----	----	----	+0.125
O(2)	----	----	----	----	----	3 <u>+0.17</u> (x3)	----	----	----	1 <u>+0.01</u>	----	----	----	+0.187
O(3)	----	----	----	----	----	----	3 <u>+0.01</u> (x3)	1 -0.02	----	----	----	----	----	+0.062
O(4)	----	1 <u>-0.23</u>	----	1 <u>+0.00</u>	----	----	----	----	----	----	----	----	1 <u>-0.03</u>	-0.333
O(5)	----	----	----	1 <u>-0.05</u>	1 <u>-0.00</u>	----	----	----	----	----	1 <u>+0.00</u>	----	----	-0.167
O(6)	----	----	----	1 <u>-0.04</u>	1 <u>+0.01</u>	----	----	----	----	1 <u>-0.00</u>	----	----	----	-0.167
O(7)	----	----	----	----	1 <u>+0.02</u>	1 <u>-0.08</u>	----	----	1 <u>+0.00</u>	----	----	----	----	-0.042
O(8)	----	----	----	----	1 <u>-0.03</u>	1 <u>-0.16</u>	----	1 <u>+0.01</u>	----	----	----	----	----	-0.105
O(9)	----	----	----	----	----	2 <u>+0.02</u> <u>+0.05</u>	1 -0.04	----	----	----	1 <u>+0.00</u>	----	----	+0.000
O(10)	----	1 <u>+0.23</u>	1 <u>+0.00</u>	----	----	----	1 <u>+0.05</u>	----	----	----	----	----	1 <u>+0.03</u>	+0.167
O(11)	1 <u>+0.04</u>	----	----	----	----	----	2 <u>-0.02</u> <u>+0.05</u>	----	----	----	----	----	1 <u>+0.01</u>	+0.000
OH(1)	1 -0.04	----	----	2 <u>-0.05</u> <u>-0.03</u>	----	----	----	----	----	----	----	----	----	+0.000
OH(2)	----	----	1 -0.00	----	----	1 <u>+0.00</u>	1 -0.05	----	----	----	----	----	----	+0.167

[†]A bond length deviation refers to the polyhedral average subtracted from the individual bond distance. The entries begin with the number of cations coordinating to an anion followed by the distance deviations. The Δp_0 = deviation of electrostatic bond strength sum from neutrality ($p_0 = 2.00$ e.s.u. for O^{2-} , 1.00 for OH^-). Bond length deviations which conform to Δp_0 are underlined.

distances usually occur toward the top of their appropriate list. It is worth noting that only the $[As^{3+}O_3]$ trigonal pyramids share edges with the larger polyhedra: all three individual trigonal pyramids involve some edge-sharing in contradistinction with the three $[T^{=4+}O_4]$ polyhedra where no edges are shared. The same phenomenon occurs in hematolite (Moore and Araki, 1978); the $As^{3+}-O$ 1.75–1.78 Å polyhedral averages are close to the 1.79 Å average in hematolite. The T–O averages steadily

increase, from T(1)–O to T(3)–O, in accordance with increasing As^{5+} solution at these sites. The O– $As^{3+}-O'$ angles range from 95° to 103°, compared with 94° in hematolite and 96° in synadelphite (Moore, 1970). Two polyhedra presented problems but these are easily resolved if extensive ordering is assumed in the dixenite structure. The M(3)–O 2.05 Å average, discussed earlier, is approximately an $Fe^{3+}-O$ distance. The M(5)–O averages show a range of distances: four distances below 2.15 Å

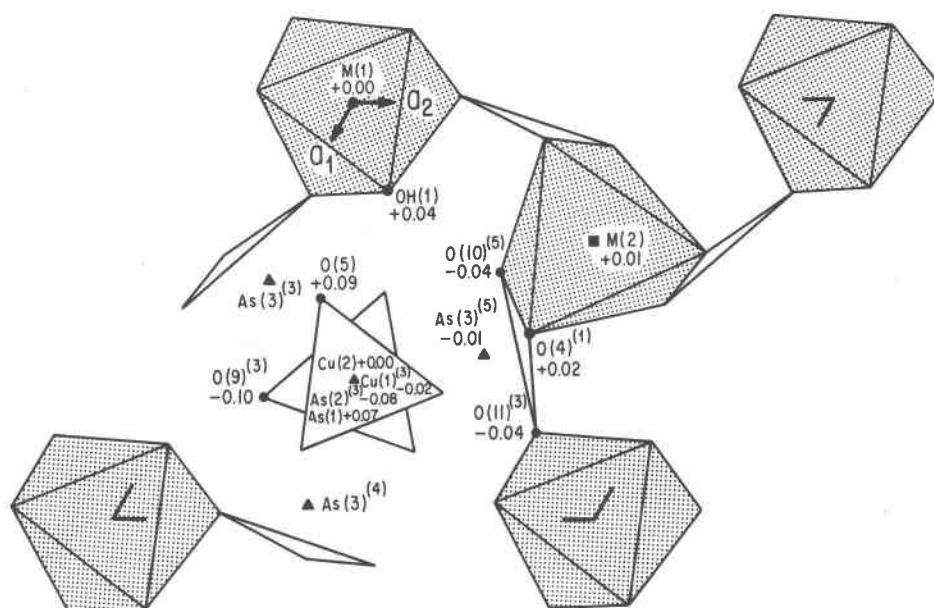


Fig. 1. Polyhedral diagrams of the five non-equivalent layers in dixenite. The layer is identified as $z = 2m/30$ where m is an integer. Heights are given as fractional coordinates.

Fig. 1a. The $m=0$ layer including the $\text{As}(1,2,3)\text{O}_3$ trigonal pyramids and the $\text{M}(2)\text{O}_6$ octahedron. This layer shows the region around the $\text{Cu}^{1+}\text{As}_4^{3+}$ cluster. Hematolite has no such layer.

(average 2.12\AA), one distance at 2.43\AA and a remaining distance at 2.73\AA . Such multiple "coordination spheres" have been noted earlier for Mn^{2+} in an oxide environment. Arsenoclasite, Mn_5^{2+}

$(\text{OH})_4(\text{AsO}_4)_2$, has polyhedra involving tetrahedral (2.13\AA average), trigonal bipyramidal (2.19\AA average) and octahedral (2.22\AA average) coordinations (Moore and Molin-Case, 1971). In the present

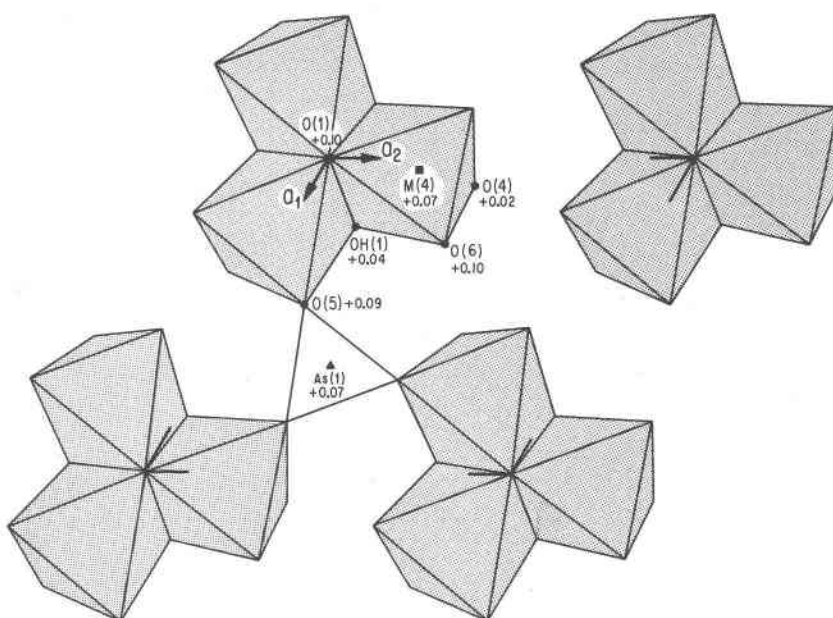


Fig. 1b. The $m=1$ layer showing the $\text{M}(4)\text{O}_6$ octahedra and the $\text{As}(1)\text{O}_3$ trigonal pyramid. This resembles the $m=2$ layer in hematolite.

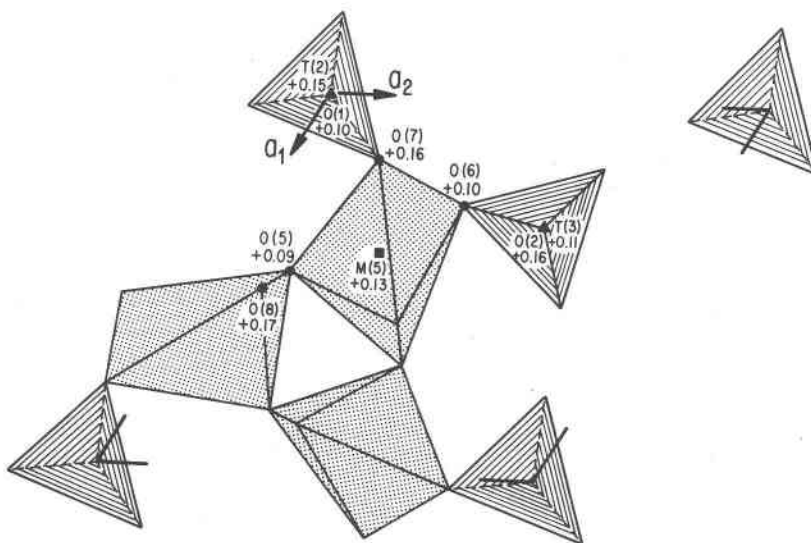


Fig. 1c. The $m=2$ layer showing the $M(5)O_4$ tetrahedron (here with additional $O(5)^{(2)}$), the $T(2)O_4$ and $T(3)O_4$ tetrahedra. Hematolite has no such layer.

study, we have chosen tetrahedral coordination of oxygens about Mn(5) and used this for the valence balance calculations in Table 7.

The $[Cu^{1+}As_3^{3+}]$ tetrahedral cluster is very interesting as discussed earlier. This cluster (Figs. 1a, 2) involving a central Cu^{1+} cation has no counterpart among the sulfosalt or arsenide structures. Besides, in dixenite the Cu atomic positions are not fully occupied but are split into two non-equivalent sites.

Mean distances (Table 5) are $Cu(1)-As(2,3)$ 2.26 and $Cu(2)-As(1,3)$ 2.40 Å. Perhaps the lautite structure contains a good model of such a cluster since Cu^{1+} is tetrahedrally coordinated by sulfur and arsenic to form a $[CuAsS_3]$ cluster. Craig and Stephenson (1965) report a $Cu-As$ 2.42 Å distance which is close to the average for the $Cu(2)As_3^{3+}$ cluster in dixenite. The short $Cu(1)As_3^{3+}$ average distance is not so easily explained. Perhaps it is a

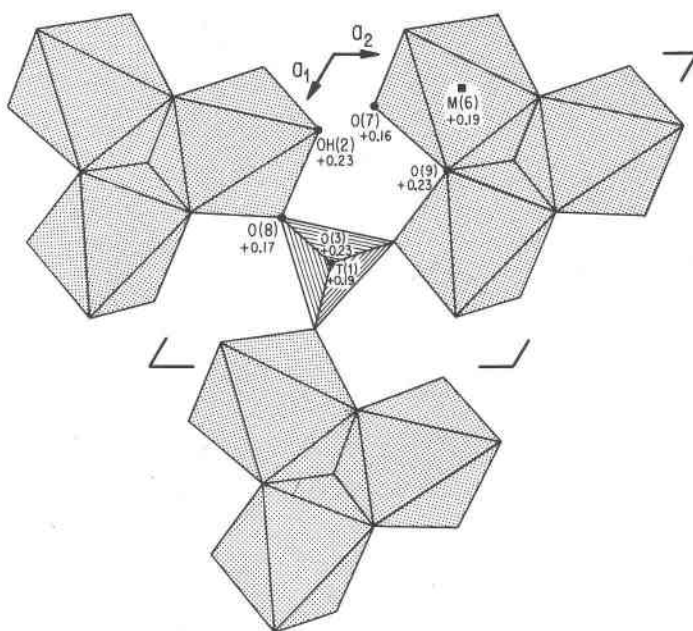


Fig. 1d. The $m=3$ layer showing the $M(6)O_6$ octahedra and the $T(1)O_4$ tetrahedron. This resembles the $m=2$ layer in hematolite.

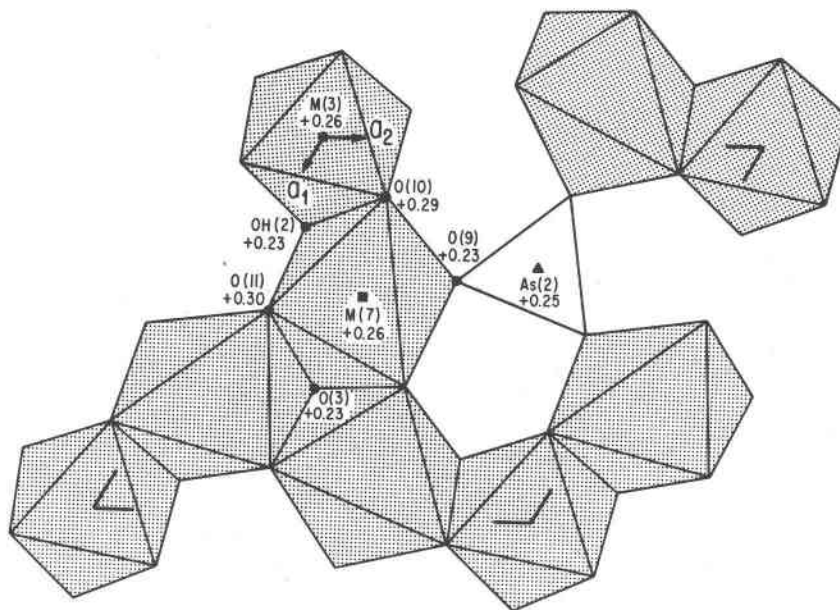


Fig. 1e. The $m=4$ layer showing the $M(3)O_6$ and $M(7)O_6$ octahedra, and the $As(2)O_3$ trigonal pyramid. This resembles the $m=1$ layer in hematolite.

consequence of the cluster disorder or even the possible presence of a different metal. This latter possibility is difficult to rationalize since there is no other site which Cu could occupy, either as Cu^{1+} (owing to its large size) or Cu^{2+} (owing to pronounced Jahn-Teller distortion).

Calculated weight percentages for the structure analytical results and for the proposed end-member formula $Cu^{1+}Mn_{14}^{2+}Fe^{3+}(OH)_6(AsO_3)_5(SiO_4)_2(AsO_4)$ show generally good agreement with Johansson's analysis of the mineral in Table 6, bearing in mind that some solid solution exists between Si^{4+} and

Table 8. Dixenite: calculated and observed powder patterns[†]

I(calc)	d(calc)	hkl	I(obs)	d(obs)
7	12.500	003	30	12.5
5	6.996	101	16	6.99
9	6.250	006	35	6.22
21	4.112	110	90	4.10
29	3.906	113	50	3.90
44	3.435	116	40	3.42
16	3.318	10.10	45	3.31
36	2.965	027	80	2.96
100	2.927	119	100	2.92
24	2.835	208	50	2.83
15	2.685	211	40	2.68
11	2.664	122	30	2.66
5	2.587	214	20	2.58
6	2.582	02.10		
7	2.533	125	16	2.53
7	2.507	01.14		
6	2.500	00.15		
25	2.488	11.12	40b	2.49
22	2.405	217	55	2.40
21	2.374	300	80	2.37
16	2.334	128	45	2.33
5	1.972	131	25	1.967
6	1.968	21.13		
5	1.820	318	12b	1.819
14	1.768	21.16	30	1.764
9	1.721	30.15	20	1.719
12	1.706	12.17	25	1.703
5	1.638	11.21	12	1.635
6	1.563	327	16	1.560
19	1.554	410	55	1.551
6	1.543	238	25b	1.541
5	1.538	12.20		

[†]The calculated data are from the refined structure, based on $CuK\alpha$ radiation. These results are compared with ASTM Powder File No. 19-426. Only calculations with $I(\text{calc}) > 5$ are listed. Agreement is good, excepting preferred orientation effects in the experimental study.

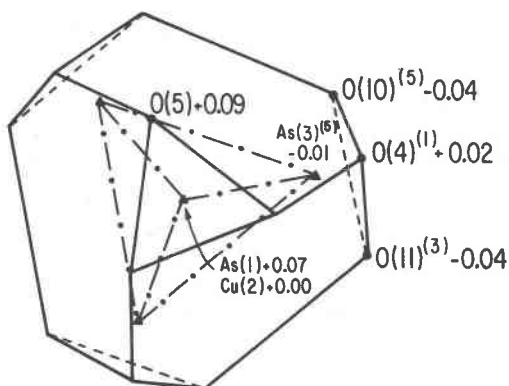


Fig. 2. The oxygen coordination polyhedron about the $Cu^{1+}As_3^{3+}$ cluster in dixenite. This polyhedron is a distorted truncated tetrahedron.

As⁵⁺. Performing the appropriate valence conversions suggested by the structure study brings Johansson's analysis into very good agreement indeed (columns 4 and 5). It is gratifying to see that very little Mn³⁺ evidently occurs in the structure, conforming to the rather reduced state of the species.

When a complex structure is well-refined it is desirable to calculate a powder pattern and compare it with existing powder data as given in Table 8. One advantage is the correct assignment of the Miller indices and its advantage over experimentally determined powder patterns which usually exhibit some preferred orientation and absorption effects.

Acknowledgment

We appreciate support of this study through the National Science Foundation grant EAR 79-18529 (Geochemistry).

References

- Burnham, C. W. (1966) Computation of absorption corrections, and the significance of the end effect. *American Mineralogist*, 51, 159-167.
- Craig, D. C. and Stephenson, N. C. (1965) The crystal structure of lautite, CuAsS. *Acta Crystallographica*, 19, 543-547.
- Cromer, D. T. and Liberman, D. (1970) Relativistic calculation of anomalous scattering factors for X-rays. Los Alamos Scientific Laboratory, University of California Report LA-4403, University of California-34.
- Cromer, D. T. and Mann, J. B. (1968) X-ray scattering factors computed from numerical Hartree-Fock wave-functions. *Acta Crystallographica*, A24, 321-324.
- Flink, G. (1920) Trigonit och dixenit, två nya mineral från Långbanshytte gruvor. *Geologiska Föreningens Förhandlingar*, 42, 436-439.
- Horiuchi, H., Morimoto, N., Yamamoto, K. and Akimoto, S.-I. (1979) Crystal structure of 2Mg₂SiO₄ · 3Mg(OH)₂, a new high-pressure structure type. *American Mineralogist*, 64, 593-598.
- Howells, E. R., Phillips, D. C. and Rogers, D. (1950) The probability distribution of X-ray intensity. II. Experimental investigation on the X-ray detection of center of symmetry. *Acta Crystallographica*, 3, 210-214.
- Moore, P. B. (1970) Crystal chemistry of the basic manganese arsenates. IV. Mixed arsenic valences in the crystal structure of synadelphite. *American Mineralogist*, 55, 2023-2037.
- Moore, P. B. and Araki, T. (1976) A mixed-valence solid solution series: crystal structures of phosphoferrite and kryzhanovskite. *Inorganic Chemistry*, 15, 316-321.
- Moore, P. B. and Araki, T. (1978) Hematolite: a complex dense-packed sheet structure. *American Mineralogist*, 63, 150-159.
- Moore, P. B. and Araki, T. (1979a) Magnussonite, manganese arsenite, a fluorite derivative structure. *American Mineralogist*, 64, 390-401.
- Moore, P. B. and Araki, T. (1979b) Armangite, Mn₂₆[As₆³⁺(OH)₄O₁₄][As₆³⁺O₁₈]₂[CO₃], a fluorite derivative structure. *American Mineralogist*, 64, 748-757.
- Moore, P. B. and Ito, J. (1978) Kraisslite, a new platy arsenosilicate from Sterling Hill, New Jersey. *American Mineralogist*, 63, 938-940.
- Moore, P. B. and Molin-Case, J. A. (1971) Crystal chemistry of the basic manganese arsenates: V. Mixed manganese coordination in the atomic arrangement of arsenoclasite. *American Mineralogist*, 56, 1539-1552.
- Wickman, F. E. (1951) From the notes of the late K. Johansson: VII. A revised chemical analysis of dixenite from Långban. *Geologiska Föreningens Förhandlingar*, 73, 637-638.
- Wuensch, B. J. (1960) The crystallography of mcgovernite, a complex arsenosilicate. *American Mineralogist*, 45, 937-945.

*Manuscript received, March 17, 1981;
accepted for publication, July 13, 1981.*